# CHAPTER 6

## 6. Development and Evaluation of Compositions: *In-vitro* and *In-vivo* Studies

### 6.1. *In-vitro* studies

Drug combinations are used to achieve synergistic therapeutic effect, dose and toxicity reduction, and to minimize or delay the induction of drug resistance. Effect based strategy is a method in which combined effect of two drugs can be directly compared with the effect of individual drugs. This strategy utilizes the combination index (CI) and isobologram methods [1].

CI was introduced to quantitatively depict synergism (CI < 1), additive effect (CI = 1), and antagonism (CI > 1). CI is calculated to show the positive drug combination effect that occurs when the observed combination effect ($E_{AB}$) is greater than the expected additive effect given by the sum of the individual effects ($E_A + E_B$).

$$CI = \frac{(E_A + E_B)}{E_{AB}} \quad \ldots.\textbf{(10)}$$

Advantage of this method is that it provides complement to the algebraic analysis with an accepted graphical approach [2,3].

On the other hand, Isobologram method is used to define the potency ratio as the dose ratio of two drugs when the same drug effect is achieved. The two drugs are prepared using a gradient dose (at least four doses) to determine the $ED_{50}$ value of the mixture ($ED_{50}$ is the dose of a compound that achieves 50% efficacy). The potency ratio ($R_B$) of drugs A and B can be calculated using following equation

$$R_B = \frac{ED_{50;A}}{ED_{50;B}} \quad \ldots.\textbf{(11)}$$

This method is also known as contour method, that has been proven mathematically. It is used as the basis for the development of most methods that are currently available [4].Using these two methods the combination studies were further designed. From the preliminary screening results, nine extracts (TAM-SO, CZW-SO, OGM-SO, GSM-SO, AVH-SX, BARM-SO, AMM-SO, PLM-SO, and TSM-SO) were found to be potent for PL inhibition. These above potent nine plant extracts were further selected for the combination studies. Compositions were prepared using two extracts at a time. Thirty-six possible compositions were designed using combinations of two extracts and were screened for PL inhibition (**Table 7**).

**Table 7**: Composition screened for PL inhibition

| Sl no. | Composition | Combination of | $IC_{50EXT1}/2 + IC_{50EXT2}/2$ | |
|---|---|---|---|---|
| | | | % Inhibition | Combination index (CI) |
| **1.** | TAM-GSM | TAM-SO+GSM-SO | 34.98± 0.98 | 1.98 |
| **2.** | AMM-PLM | AMM-SO+PLM-SO | 59.77± 0.32 | 0.91 |
| **3.** | BARM-GSM | BARM-SO + GSM-SO | 80.35± 0.65 | 0.52 |
| **4.** | TAM-OGM | TAM-SO+OGM-SO | 23.09± 1.12 | 1.08 |
| **5.** | TAM-CZW | TAM-SO+CZW-SO | 39.56± 0.99 | 1.67 |
| **6.** | TAM-BARM | TAM-SO+BARM-SO | 21.12± 0.23 | 1.11 |
| **7.** | TAM-AMM | TAM-SO+AMM-SO | 25.87± 0.67 | 2.09 |
| **8.** | OGM-GSM | OGM-SO+GSM-SO | 32.09± 0.98 | 1.65 |
| **9.** | OGM-BARM | OGM-SO+BARM-SO | 37.54± 0.87 | 1.98 |
| **10** | OGM-AVH | OGM-SO+AVH-SX | 22.34± 1.23 | 1.76 |
| **11** | OGM-AMM | OGM-SO+AMM-SO | 37.76± 2.12 | 2.11 |
| **12.** | GSM-PLM | GSM-SO+PLM-SO | 33.98± 1.43 | 1.54 |
| **13.** | GSM-AVH | GSM-SO+AVH-SX | 38.22± 0.76 | 1.12 |
| **14.** | GSM-AMM | GSM-SO+AMM-SO | 24.98± 0.99 | 1.56 |
| **15.** | CZW-OGM | CZW-SO+OGM-SO | 44.91± 0.98 | 1.87 |
| **16.** | CZW-GSM | CZW-SO+GSM-SO | 39.56± 0.54 | 1.98 |
| **17.** | CZW-BARM | CZW-SO+BARM-SO | 33.12± 0.43 | 1.55 |
| **18.** | CZW-AVH | CZW-SO+AVH-SX | 37.34± 0.78 | 1.45 |
| **19.** | CZW-AMM | CZW-SO+AMM-SO | 28.54± 1.12 | 1.87 |
| **20.** | BARM-PLM | BARM-SO+PLM-SO | 41.66± 1.32 | 2.65 |
| **21.** | BARM-AMM | BARM-SO+AMM-SO | 36.09± 0.76 | 1.04 |
| **22.** | AVH-BARM | AVH-SX+BARM-SO | 20.89± 0.54 | 1.98 |
| **23.** | AVH-AMM | AVH-SX+AMM-SO | 24.68± 0.99 | 2.09 |
| **24.** | TAM-AVH | TAM-SO+AVH-SX | 35.65± 1.12 | 1.12 |
| **25.** | TAM-PLM | TAM-SO+PLM-SO | 40.25± 0.56 | 1.39 |
| **26.** | CZW-PLM | CZW-SO+PLM-SO | 32.45± 2.45 | 1.23 |
| **27.** | OGM-PLM | OGM-SO+PLM-SO | 38.12± 0.56 | 1.43 |
| **28.** | AVH-PLM | AVH-SX+PLM-SO | 37.90± 0.45 | 2.06 |
| **29.** | TAM-TSM | TAM-SO+TSM-SO | 42.87± 0.65 | 1.32 |
| **30.** | CZW-TSM | CZW-SO+TSM-SO | 30.00± 0.33 | 1.65 |
| **31.** | OGM-TSM | OGM-SO+TSM-SO | 30.46± 0.87 | 1.39 |
| **32.** | AVH-TSM | AVH-SX+TSM-SO | 23.43± 0.45 | 1.98 |
| **33.** | BARM-TSM | BARM-SO+TSM-SO | 70.86± 0.54 | 0.73 |
| **34.** | AMM-TSM | AMM-SO+TSM-SO | 46.76± 2.54 | 2.45 |
| **35.** | GSM-TSM | GSM-SO+TSM-SO | 60.21± 0.23 | 0.77 |
| **36.** | PLM-TSM | PLM-SO+TSM-SO | 38.74± 1.87 | 1.56 |

All experiments were performed in triplicate (n = 3). All the values are expressed as mean± S.E.M

Out of these 36 compositions, only 4 showed synergistic interactions. The synergistic PL inhibitory compositions are as follow:

a. Ultrasound assisted methanol extracts of *B. aristata* and *G. sylvestre* (BARM-GSM)
b. Ultrasound assisted methanol extracts of *B. aristata* and *T. sinensis* (BARM-TSM)
c. Ultrasound assisted methanol extracts of *G. sylvestre* and *T. sinensis* (GSM- TSM)
d. Ultrasound assisted methanol extract of *A. marmelos* and *P. longum* (AMM-PLM)

The detailed studies of these 4 compositions were further performed using CI and isobologram methods.

### 6.1.1 Combination studies of BARM-SO and GSM-SO (BARM-GSM)

To assess the synergistic interaction potential of BARM-SO with GSM-SO, five combinations for BARM-SO with GSM-SO were prepared and evaluated for their PL inhibition potential. The concentrations of BARM-SO (0, $IC_{50}/8$, $IC_{50}/4$, $IC_{50}/2$ and $IC_{50}$) and GSM-SO (0, $IC_{50}/8$, $IC_{50}/4$, $IC_{50}/2$ and $IC_{50}$) were mixed in a constant ratio **(Figure 21)**. Experiments and data analysis were performed as mentioned in Chapter 4 (Section 4.4 and 4.5) [5].

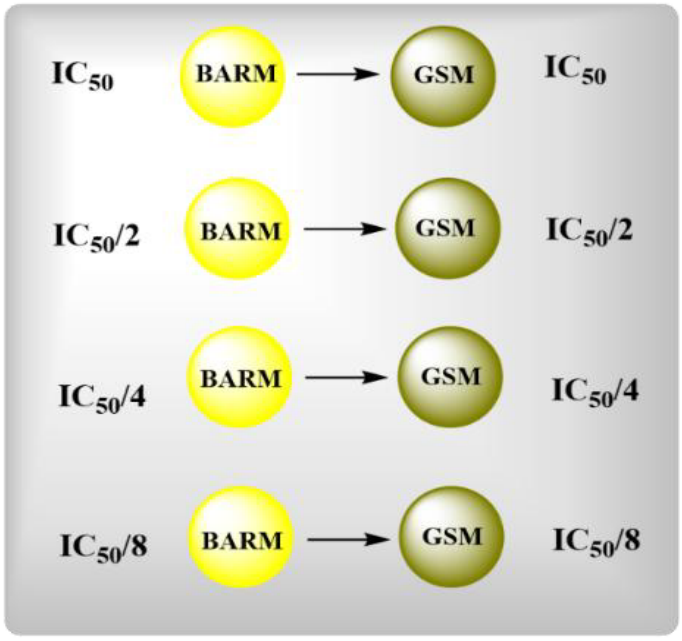


**Figure 21:** Basic approach to develop BARM-GSM

Combination index was analyzed using CompuSyn® software. In CompuSyn® software, the dose represented the combinational concentration of both the extracts and the effect was depicted

as Fa ($0 < Fa < 1$), i.e. the inhibition percentage of PL. According to the Fa value, its corresponding CI value was obtained. For synergistic effect, CI<1; for additive effect CI = 1, while for antagonistic effect CI > 1 were considered [2]. In Isobologram approach, the $IC_{50}$ values of the both extracts were plotted on the *y* and *x*- axis in a two-coordinate plot, that corresponded to (0, $IC_{50,EXT1}$) and (0, $IC_{50,EXT2}$), respectively. The line connecting these two points indicated the line of additivity. If the co-ordinate points (concentration of EXT1 and EXT2 in $IC_{50}$ of the combination) were located below the line of additivity, then it represented the synergistic mechanism between the two extracts. If the co-ordinate points were located on the line the additive effect existed, while antagonistic effect was designated when the points were found above the line [4].

BARM-SO and GSM-SO exhibited a dose-dependent PL inhibition. BARM-SO exhibited an $IC_{50}$ of 11.10 µg/ml in PL inhibition assay, while GSM-SO showed $IC_{50}$ of 7.57 µg/ml. In CompuSyn® software, the Fa values for the BARM- GSM composition were 0, 0.42, 0.51, 0.62 & 0.80, when the concentrations of BARM-SO were 0, 1.39, 2.77, 5.55 & 11.10 µg/ml and the concentrations of GSM-SO were 0, 0.95, 1.89, 3.79 & 7.57 µg/ml, respectively **(Figure 22A)**. According to the Fa value, its corresponding CI values (0, 0.95, 0.73, 0.52 & 0.33) were obtained. The above results indicated the synergistic interaction between these two extracts **(Figure 22B)**. Further, the synergistic interaction between these extracts was validated using the isobologram method. Similar results were observed in this method wherein the concentrations of the two extracts in the combination were located below the line of additivity **(Figure 22C)**. The combined $IC_{50}$ of the composition ($cIC_{50}$) was found to be 5.05 ± 1.05 µg/ml in which the concentration of BARM-SO and GSM-SO was 3.44 and 1.61 µg/ml, respectively. The results of the two methods proved the synergistic interactions of the above two extracts.

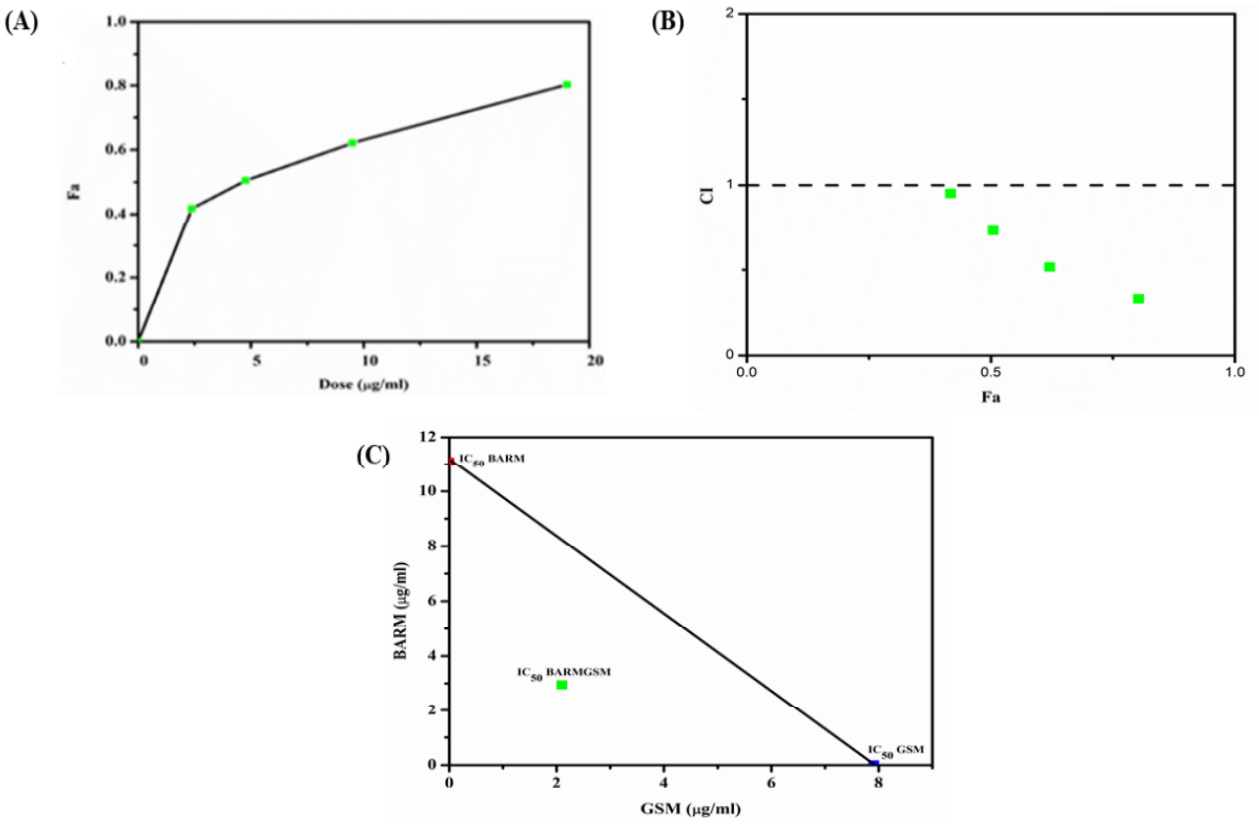


**Figure 22:** Combination studies of BARM-SO and GSM-SO (A) Dose-effect curve of BARM-GSM for PL inhibition; (B) Combination index plot of BARM-SO and GSM-SO; (C) Isobologram plot of BARM-SO and GSM-SO

### 6.1.2 Combination studies of BARM-SO and TSM-SO (BARM-TSM)

The $IC_{50}$ values of BARM-SO and TSM-SO were obtained from the dose-dependent inhibition curve. The concentrations of BARM-SO (0, $IC_{50}/8$, $IC_{50}/4$, $1/IC_{50}/2$ and $IC_{50}$) and TSM-SO (0, $IC_{50}/8$, $1/IC_{50}/4$, $1/IC_{50}/2$ and $IC_{50}$) were mixed in a constant ratio **(Figure 23)**. The combined inhibition effect on PL was determined using the method as discussed above section.

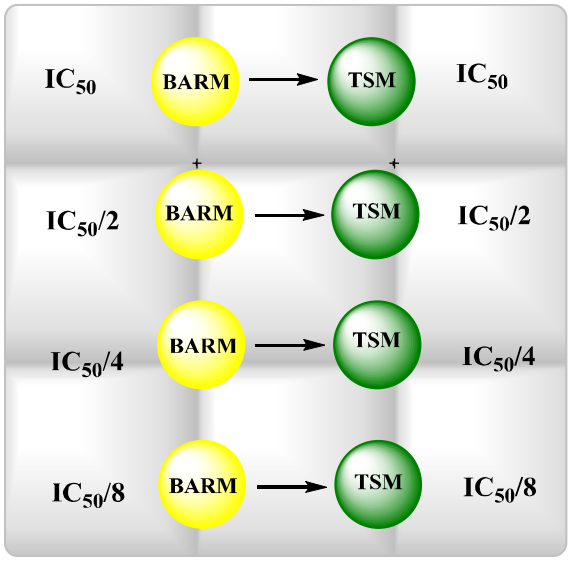


**Figure 23:** Basic approach to develop BARM-TSM

BARM-SO exhibited an $IC_{50}$ of 11.10 µg/ml in the PL inhibition assay, while TSM-SO possessed an $IC_{50}$ of 20.00 µg/ml. To assess the synergistic potential of BARM-SO with TSM-SO, five combinations for BARM-SO with TSM-SO were prepared and evaluated for their PL inhibition activity. The obtained activity of the combination, as well as the individual activity of both the extracts, were incorporated into the CompuSyn® software, to retrieve the CI values [6]. In CompuSyn® software, the dose represented the combinational concentration of both the extracts and the effect was depicted as Fa ($0 < Fa < 1$), i.e. the inhibition percentage of PL. The Fa values for the BARM-TSM composition were 0, 0.41, 0.58, 0.71 & 0.82 when the concentrations of BARM-SO were 0, 1.39, 2.77, 5.55 & 11.10 µg/ml and the concentrations of TSM-SO were 0, 2.50, 5.00, 10.00 & 20.00 µg/ml, respectively **(Figure 24A)**. According to the Fa value, its corresponding CI values (0, 1.72, 0.91, 0.74, 0.66) were obtained **(Figure 24B)**. Further, the synergistic interaction between these extracts was validated using the isobologram method. Similar results were observed in this method wherein the concentrations of the two extracts in the combination were located below the line of additivity **(Figure 24C)**. The $cIC_{50}$ of the composition was found to be 10.63 ± 0.59 µg/ml in which the concentration of BARM-SO and TSM-SO was 3.605 and 7.025 µg/ml, respectively. The results of the two methods used proved the synergistic interactions of the above two extracts.

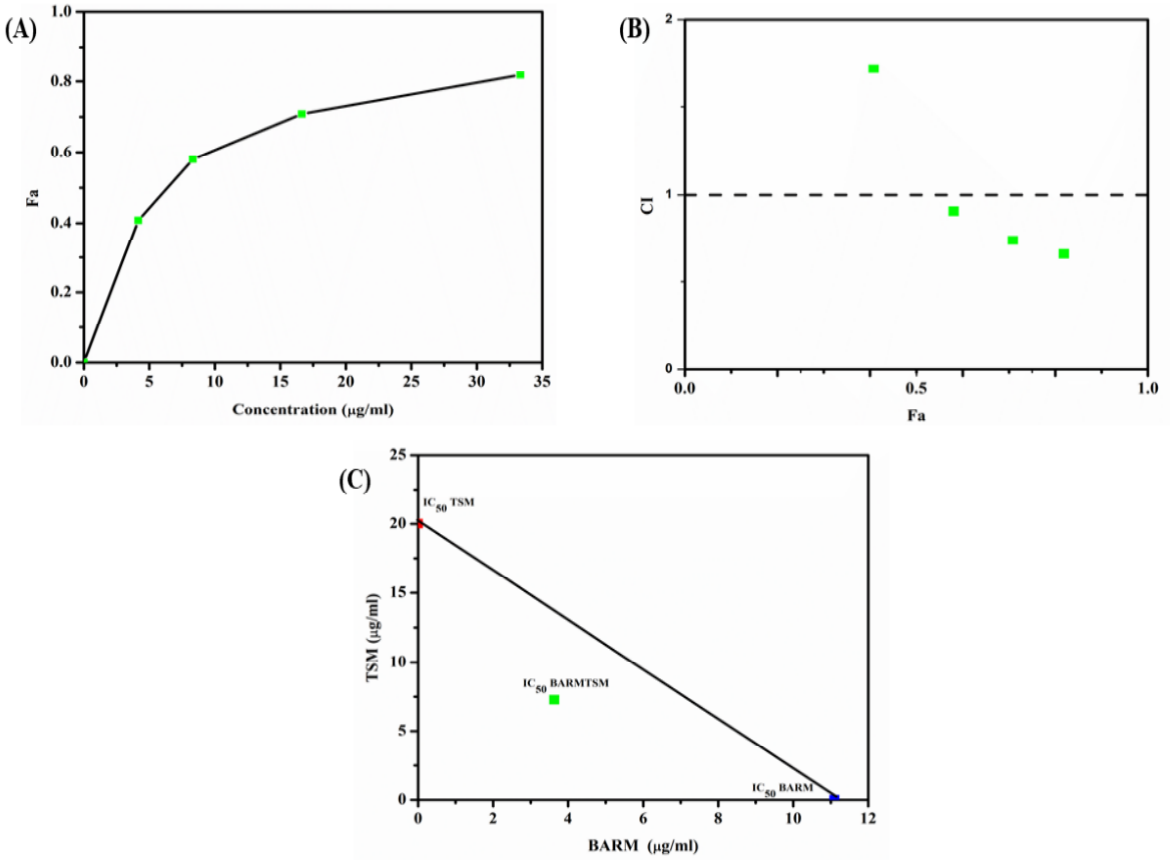


**Figure 24:** Combination studies of BARM-SO and TSM-SO (A) Dose-effect curve of BARM-TSM for PL inhibition; (B) Combination index plot of BARM-SO and TSM-SO; (C) Isobologram plot of BARM-SO and TSM-SO

### 6.1.3 Combination studies of GSM-SO and TSM-SO (GSM-TSM)

The $IC_{50}$ values of GSM-SO and TSM-SO were obtained from the dose-dependent inhibition curve. The concentrations of GSM-SO (0, $IC_{50}/8$, $1/IC_{50}/4$, $1/IC_{50}/2$ and $IC_{50}$) and TSM-SO (0, $IC_{50}/8$, $1/IC_{50}/4$, $1/IC_{50}/2$ and $IC_{50}$) were mixed in a constant ratio **(Figure 25)**. The combined inhibition effect on PL was determined using the method as discussed above.

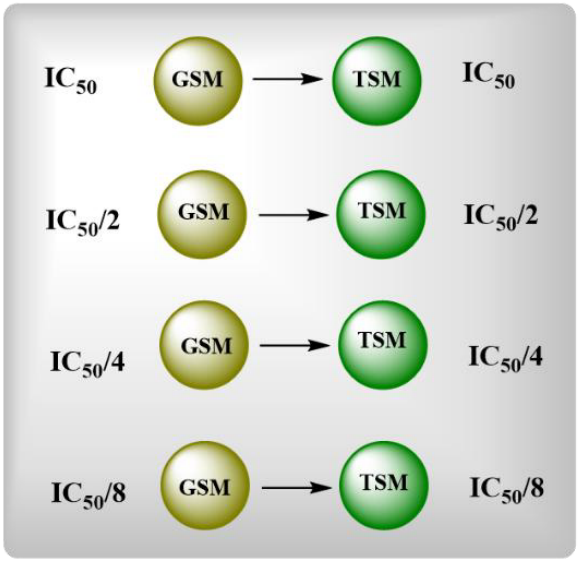


**Figure 25:** Basic approach to develop GSM-TSM

GSM -SO exhibited an $IC_{50}$ of 7.57 µg/ml individually in PL inhibition assay, while TSM-SO showed $IC_{50}$ of 20.00 µg/ml. Synergistic potential of GSM-SO with TSM-SO, were assessed by using five combinations for GSM-SO and TSM-SO and evaluated for their PL inhibition activity. The obtained activity of the combination, as well as the individual activity of both the extracts, were incorporated into the CompuSyn® software, to retrieve the CI values.

The Fa values for the GSM-TSM composition were 0, 0.34, 0.49, 0.60 and 0.73 when the concentration of GSM-SO were 0, 0.95, 1.89, 3.79 & 7.57 µg/ml and the concentrations of TSM-SO were 0, 2.50, 5.00, 10.00 & 20.00 µg/ml, respectively **(Figure 26A)**. According to the Fa value, its corresponding CI values (0. 2.01, 1.26, 0.77, 0.34) were obtained **(Figure 26B)**. Further, the synergistic interaction between these extracts was validated using the isobologram method. Similar results were observed in this method wherein the concentrations of the two extracts in the combination were located below the line of additivity **(Figure 26C)**. The $cIC_{50}$ of the composition was found to be 11.49 ± 0.45 µg/ml in which the concentration of GSM-SO and TSM-SO was 3.50 and 7.99 µg/ml, respectively. The results of the above two methods used proved the synergistic interaction of the above two extracts.

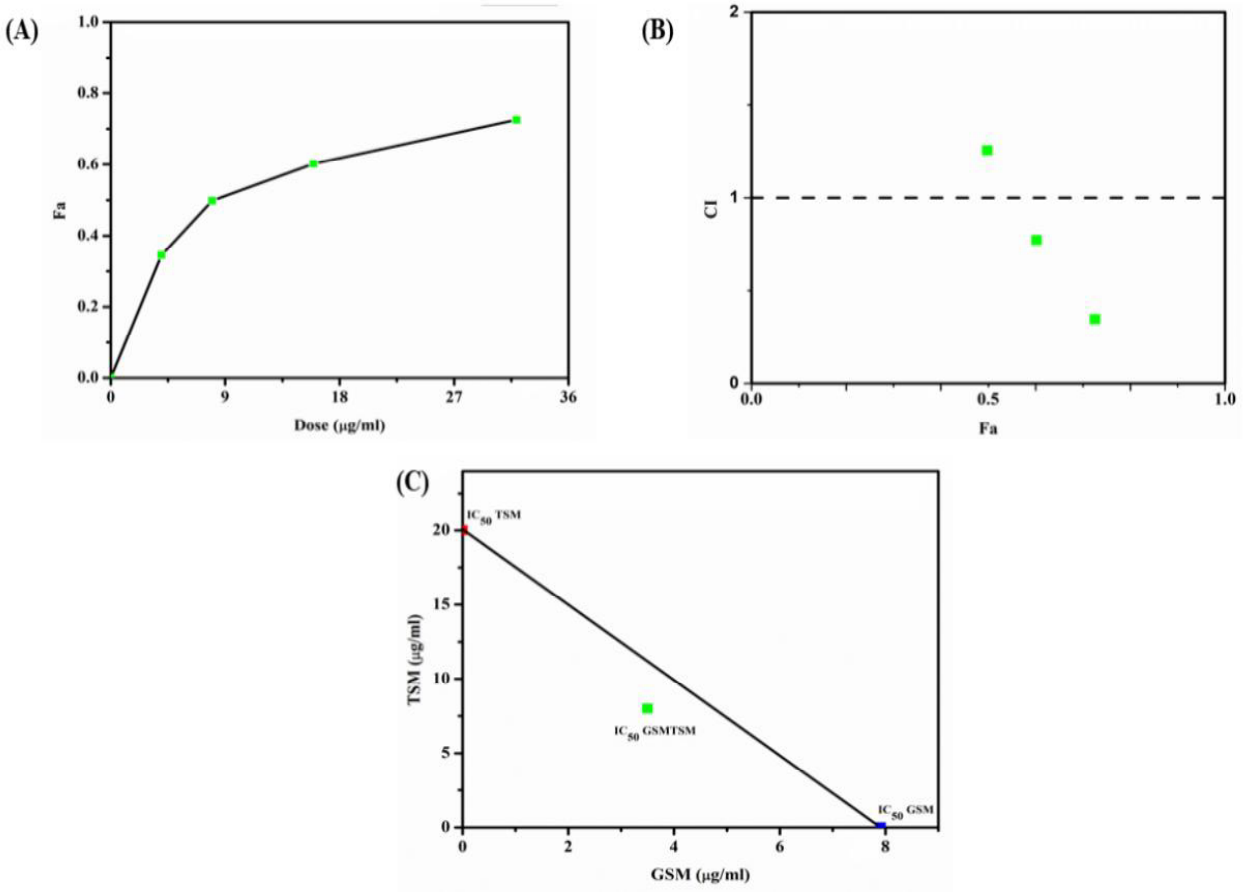


**Figure 26:** Combination studies of GSM-SO and TSM-SO (A) Dose-effect curve of GSM-TSM for PL inhibition; (B) Combination index plot of GSM-SO and TSM-SO; (C) Isobologram plot of GSM-SO and TSM-SO

### 6.1.4 Combination studies of AMM-SO and PLM-SO (AMM-PLM)

The $IC_{50}$ values of AMM-SO and PLM-SO were obtained from the dose-dependent inhibition curve. The concentrations of AMM-SO (0, $IC_{50}$/8, 1/$IC_{50}$/4, 1/$IC_{50}$/2 and $IC_{50}$) and PLM-SO (0, $IC_{50}$/8, 1/$IC_{50}$/4, 1/$IC_{50}$/2 and $IC_{50}$) were mixed in a constant ratio **(Figure 27)**. The combined inhibition effect on PL was determined using the method as discussed above.

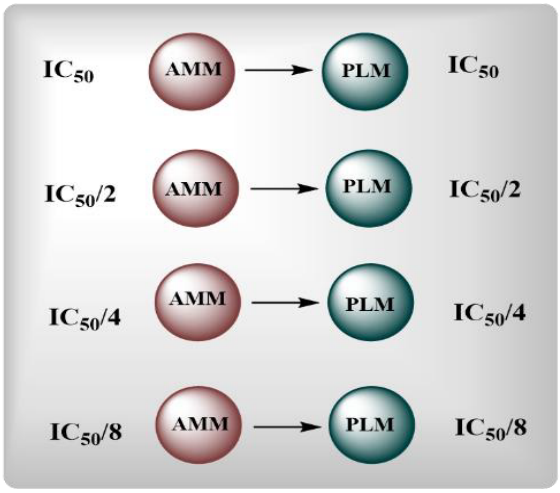


**Figure 27:** Basic approach to develop AMM-PLM

AMM -SO possessed an $IC_{50}$ of 13.02 µg/ml in the PL inhibition assay, while PLM-SO exhibited $IC_{50}$ of 14.10 µg/ml. To assess the synergistic potential of AMM-SO with PLM-SO, five combinations for AMM-SO with PLM-SO were prepared and evaluated for their PL inhibition potential. The obtained $IC_{50}$ value of the AMM-PLM composition, as well as the individual $IC_{50}$ of both the extracts were incorporated into the CompuSyn® software, to retrieve the CI values.

The Fa values for the AMM-PLM composition were 0, 0.37, 0.44, 0.50 & 0.51 when the concentrations of AMM-SO were 0, 1.63, 3.25, 6.51 & 13.02 µg/ml and the concentration of PLM-SO were 0, 1.76, 3.53, 7.05 & 14.10 µg/ml, respectively **(Figure 28A)**. According to the Fa values, its corresponding CI values (0, 1.76, 0.87, 0.91, 0.99) were obtained. For synergistic effect, CI<1, while, for additive effect CI = 1 and antagonistic effect CI > 1 **(Figure 28B)**. Further, the synergistic interaction between these extracts was validated using the isobologram method. Similar results were observed in this method wherein the concentrations of the two extracts in the combination were located on the line of additivity **(Figure 28C)**. The $cIC_{50}$ of the composition was found to be 13.55 ± 0.21 µg/ml in which the concentration of AMM-SO and PLM-SO was 6.5 and 7.05 µg/ml, respectively. The results of the above two methods used proved the additive interaction of the above two extracts.

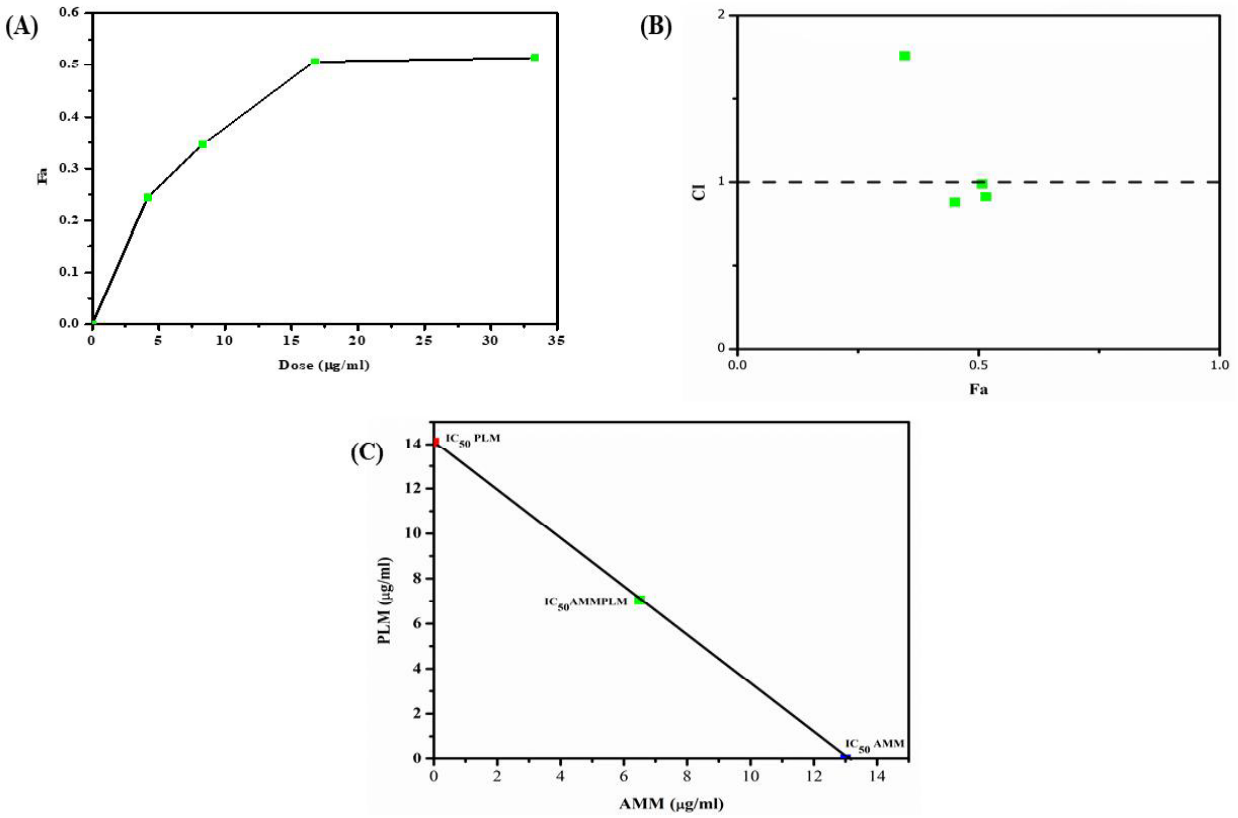


**Figure 28:** Combination studies of AMM-SO and PLM-SO (A) Dose-effect curve of AMM-PLM for PL inhibition; (B) Combination index plot of AMM-SO and PLM-SO; (C) Isobologram plot of AMM-SO and PLM-SO

### 6.2 *In vivo* Studies

Based on the *in vitro* results ($cIC_{50}$ value), two best compositions namely BARM-GSM and BARM-TSM were considered for *in vivo* experiments.

There are various polygenic diet-induced animal models used for screening of drugs against obesity. Diet induced animal model was selected as the plant extracts and their combinations were screened for PL inhibition. PL is released when food rich in triglyceride reaches duodenum for absorption. There are numerous such types of models that have designed to screen PL inhibitors. Some of them are as follow:

1. Diet-induced obesity (DIO) rat model
2. Cafeteria induced obesity model
3. High-fat diet (HFD) model
4. Early postnatal overfeeding animal models

Amongst all the models, HFD induced models are most common as fat composition plays a key role in development of obesity. Thus, HFD have similar effects on lean as well as diet resistant animals. Such effect is contributed as the caloric density of HFD, and intake of total energy is higher. This rapidly and specifically reduce the central actions of insulin and leptin most likely due to a post-receptor effect. Therefore, HFD induced obesity in Swiss albino mice was used to screen the above PL inhibitory compositions [7].

### 6.2.1 Determination of dose

*G. sylvestre* and *T. sinensis* have been previously reported to inhibit PL in *in vivo* studies. Dose of the individual extracts (GSM-SO & TSM-SO) were determined from the previous reports. Toxicity studies of saponin-rich fraction of *G. sylvestre* obtained from aqueous leaf extract have been studied. Toxicity and mortality have been observed between 800 - 2000 mg/kg dose in Wistar rats [8]. In another reports, 500 mg/kg of *G. sylvestre* aqueous leaf extract was used as dose in ICR mice model of obesity [9]. Based on the above reports, it was deemed fit to use 500 mg/kg as the high dose, while 250 mg/kg was selected as low dose. Similarly, there are reports that suggests that green tea reduced obesity at 1000 mg/kg dose in ICR mice model [10]. However, the toxicity studies suggested that after 14 weeks of continuous administration with 1000 mg/kg may develop abnormal breathing, ataxia, and early deaths in the treatment group. Such observation was specific to female mice [11]. Hence, in case of *T. sinensis* 1000 mg/kg was selected as high dose and 500 mg/kg as low dose. No direct reports are available on the dose of *B. aristata* for treatment of obesity. However, doses of berberine (75 mg/kg) [12] and palmatine (40 mg/kg) [13,14] have been individually reported for obesity treatment in mice. The amount of bio-active markers namely berberine & palmatine (refer chapter 7 & 8) in the BARM-SO was used to calculate the dose of *B. aristata* required. The high dose calculated was 800 mg/kg and low dose considered was 400 mg/kg. Using the *in vitro* results, the synergistic ratio of the combination of two extracts were determined. The same ratio was used while considering the dose for *in vivo* study (**Figure 29**).

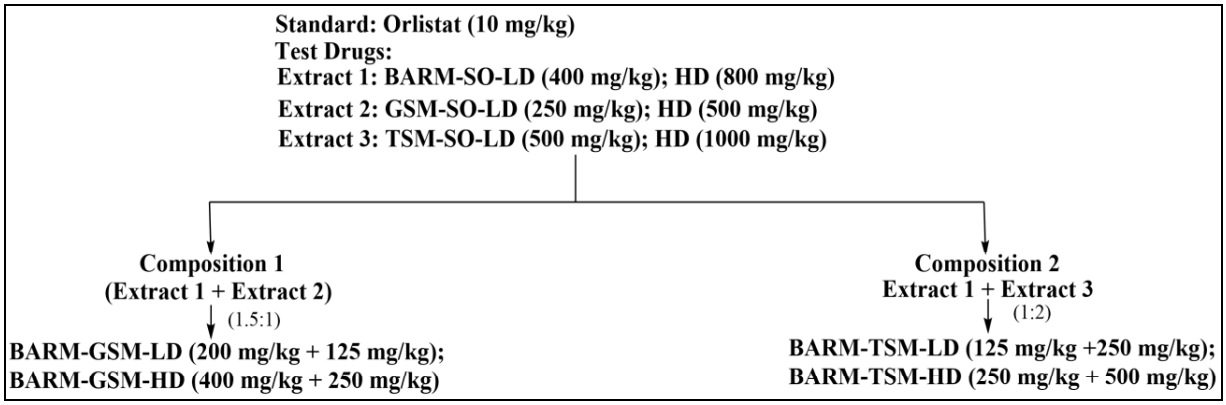


**Figure 29:** Dose considered for *in vivo* analysis

### 6.2.2 Development of HFD model

Male Swiss albino mice (22-25 g) were purchased from the Central Animal Facility (CAF) of Birla Institute of Technology and Science, Pilani, (BITS, Pilani), Pilani campus, Rajasthan (CPCSEA Reg number: 417/PO/ReBI/2001/CPCSEA). All the experimental procedures were in compliance with the Institutional Animal Ethics Committee (IAEC) of BITS Pilani (Ref: IAEC/RES/24/17/Rev-1/28/37). The mice were housed in polyacrylic cages and maintained under standard husbandry conditions (room temperature $22 \pm 1°C$ and relative humidity of 60%) with 12-h light/dark cycle. The animals were acclimatized for one week before the commencement of the experiment. After acclimatization, animals were divided into 13 groups of six animals each. Group I received normal diet (ND), while others received HFD. The animals were fed with filtered water *ad libitum*. ND was composed of 35% carbohydrates, 20% proteins, 5% fats and 10% fibres, while HFD was composed of 20% carbohydrates, 23% proteins, 47% fats and 5% fibres.

HFD mice model was developed for 3 months followed by treatment (*via* oral route) for 1 month. Treatment was initiated from the beginning of fourth month of the study and the respective dose (extracts and their compositions 1 & 2) were regularly administered for one month. Orlistat (10 mg/kg) was considered as positive control. No mortality was observed till the end of the study. Body weight were measured once in every week. Initial body weight of mice ranged from 22-25g and after continuous feeding with HFD for three months, the body weight increased to 45-50g. Blood was collected from each animal (0.2 ml) after every 15 days through retro-orbital plexus. The blood collected was centrifuged at 3000 rpm for 15 min at 4°C. Serum

was separated and used for various biochemical estimations such as TC, TG, HDL using their respective commercial biochemical kits. LDL and VLDL levels were calculated using the following equations [15]

$$LDL = [TC - \left(HDL + \left(\frac{TG}{5}\right)\right)] \quad \ldots.(12)$$

$$VLDL = [TC - (HDL + LDL) \quad \ldots.(13)$$

At the end of the study, animals were kept in metabolic cages and feces of each group were collected. The collected feces were treated using 0.15M NaCl, followed by 4:1 % *v/v* chloroform/methanol mixture. The lower organic phase was collected, filtered and dried. The TG obtained were measured using TG estimation kit. All the animals were sacrificed at the end of the experiment. Adipose tissue and liver were collected, weighed and stored in 10% buffered formalin. The samples were further processed for histopathological studies. The obtained sections of liver and adipose tissues were stained with H&E to determine the changes caused by the deposition of fat due to HFD consumption. Another section of liver was treated with picrosirius red stain to observe the collagen formation due to HFD consumption.

The body weight of mice in all the groups were similar at baseline and constantly increased over time. At the end of the 12-week experimental period [16], HFD induced a significant ($P<0.05$) increase of 33.33% in body weight of the disease control (DC) group compared to the normal control (NC) group. Liver and abdominal fat weight, which included the epididymal, visceral and mesenteric fats were significantly ($P<0.05$) higher in DC compared to NC. A 33.97% and 79.43 % of increase in weight of liver and adipose tissue, respectively were observed **(Figure 30A & B)**. During the analysis of serum lipid profile, the TC and TG level was found to be increased by 39.21% and 40.33 % respectively, while HDL level was reduced to 42.37 % in DC compared to the NC **(Figure 31)**.

**6.3 Anti-obesity effect of BARM-GSM in HFD Swiss albino mice**

High dose of BARM-GSM (400 mg/kg of BARM+ 250 mg/kg of GSM) significantly ($P<0.05$) reduced the final body weight (g), liver weight and abdominal fat deposition, when compared to the DC group. There was no significant difference observed when compared to Orlistat control

(OC) group. As represented in **Figure 30A**, the body weight of the group was reduced by 45.43% w/w. Subsequently, 53.58 and 81.56 % w/w of reduction in weight of liver and adipose tissue were observed respectively (**Figure 30B**).

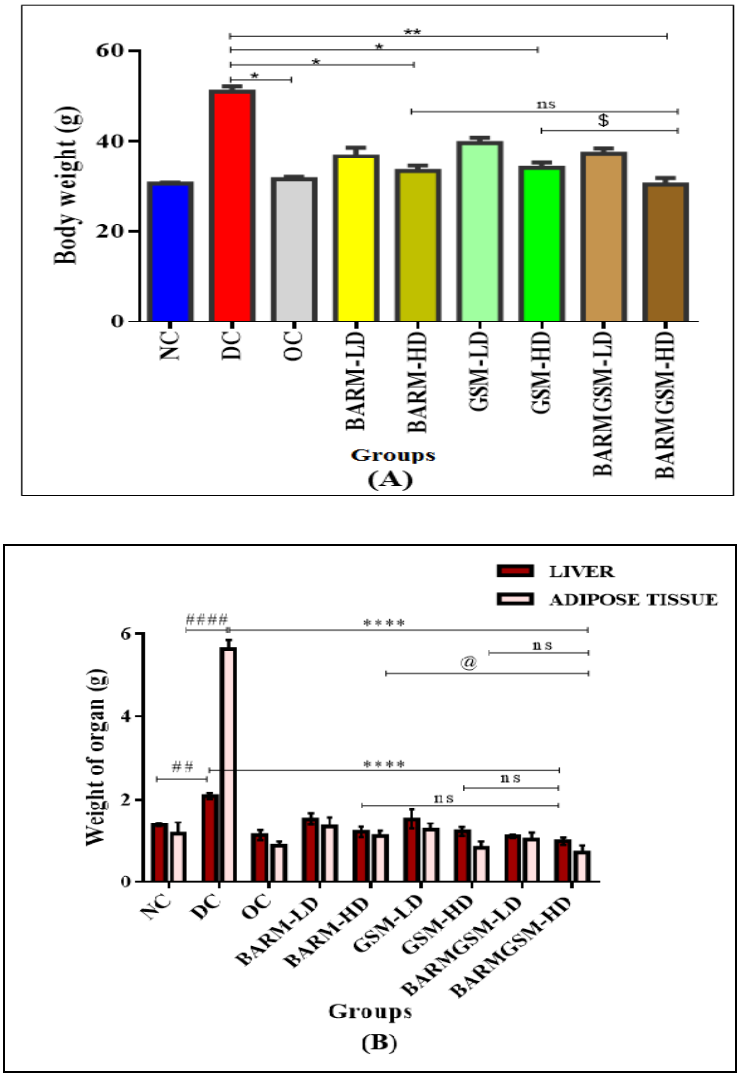


**Figure 30:** Effect of BARM-GSM on (A) bodyweight and (B) liver and abdominal fat content in mice fed with HFD. Results are reported as means ± SEM. {# *(P<0.05) Vs.* NC. **(P<0.05) Vs.* DC; *@(P<0.05) Vs.* BARM; ns*(P<0.05)* non-significant}.

Further, serum lipid profile results suggested a significant reduction in the test groups compared to the DC group, while no significant difference was observed when compared to OC group (**Figure 31**). As reported earlier, the hypocholesterolemic activity of *G. sylvestre* extract was due to increased excretion of cholesterol, neutral steroids, bile acids in the feces, and lipid-lowering

effects, resulting in decreased lipid accumulation [8]. On the other side, *B. aristata* extract conatined berberine as major constituents that was reported to reduced TC, TG and LDL cholesterol and increased HDL cholesterol after 3 months in randomized subjects [17]. In 2016, Ma *et al*, reported that palmatine reduced serum TC, TG, LDL and increased HDL levels in mice. Thus, palmatine attenuated the impaired lipid metabolism and hepatomegaly in diabetic mice [18]. BARM-GSM composition exhibited significant changes in lipid profile (decreased 43.23% of TC, 28.73% of TG and increased 47.43% of HDL levels) due to the combined effects of the phytochemicals present in both the extracts.

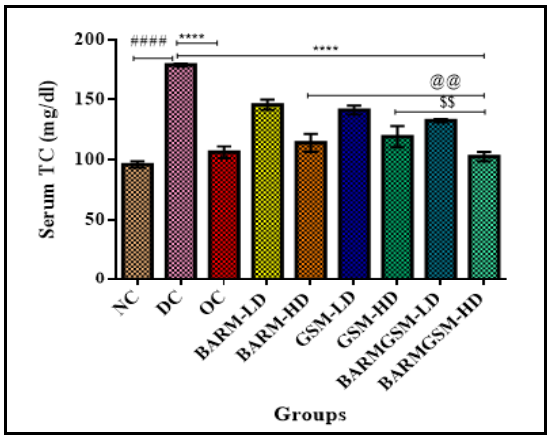


**(A)**

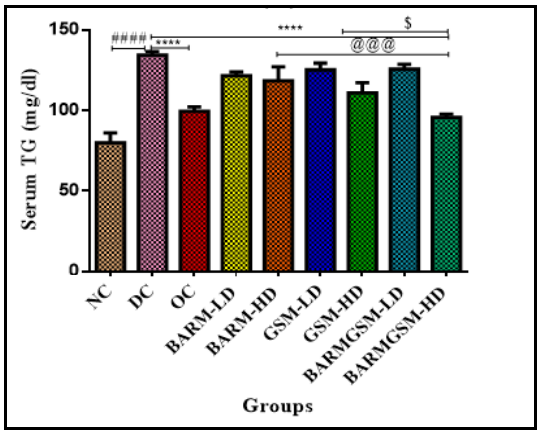


**(B)**

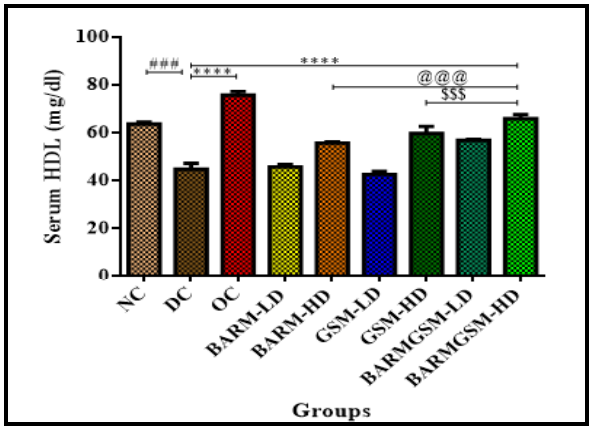


**(C)**

**Figure 31:** Effect of BARM-GSM on serum lipid profile (A) serum TC (B) serum TG and (C) serum HDL. Results are reported as means ± SEM. {*# (P<0.05) Vs.* NC; **(P<0.05) Vs.* DC; *@(P<0.05) Vs.* BARM; *$(P<0.05) Vs.* GSM; ns*(P<0.05)* non-significant}

## CHAPTER 6

The changes in the lipid profile (LDL & VLDL) after administration of BARM-GSM composition are tabulated in **Table 8.**

**Table 8:** Effect of BARM-GSM on lipid profile

| Groups | LDL (mg/dl) | VLDL (mg/dl) |
|---|---|---|
| NC | 16.37 ± 2.71 | 15.99 ± 1.72 |
| DC | 107.32 ± 1.42 | 26.86 ± 1.42 |
| OC | 12.57 ± 2.19 | 17.90± 2.59 |
| BARM-LD | 75.77 ± 3.26 | 24.31 ± 2.12 |
| BARM-HD | 34.60 ± 3.19 | 23.69 ± 1.46 |
| GSM-LD | 73.69 ± 1.99 | 25.04 ± 1.69 |
| GSM-HD | 37.34 ± 5.67 | 22.20 ± 4.41 |
| BARM-GSM-LD | 50.67 ± 1.65 | 25.11± 0.98 |
| BARM-GSM-HD | 17.59 ± 3.86 | 19.14 ± 2.51 |

Values are reported as means ± SEM (n=6)

To understand, whether BARM-GSM exhibited anti-obesity activity *via* PL inhibition, fecal TG levels were analyzed. As represented in **Figure 32**, the TG levels were significantly higher in the DC group compared to the NC group. Further, these levels increased significantly (P<0.05) with the administration of orlistat (10 mg/kg) or BARM-GSM-HD. Significant difference in fecal TG levels (P<0.05) were observed for BARM-GSM-HD treated group in comparison to OC group. Thus, the results clearly indicated that BARM-GSM exhibited potent anti-obesity potential *via* PL inhibition.

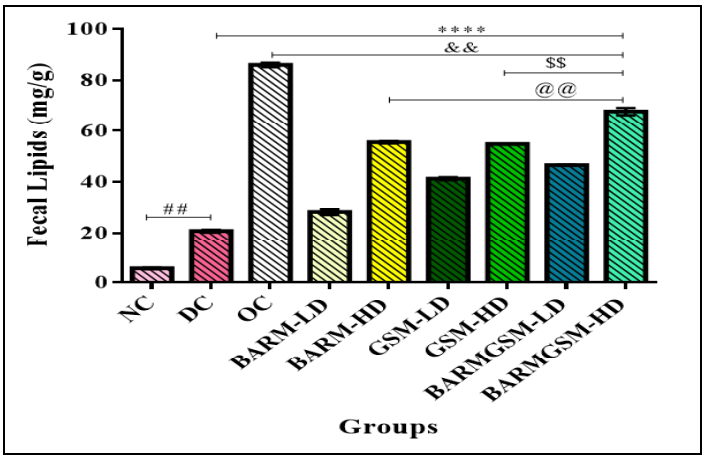


**Figure 32**: Fecal triglyceride levels determined after treatment with BARM-GSM. {*# (P<0.05) Vs.* NC; **(P<0.05) Vs.* DC; &(*P<0.05*) *Vs.* OC; *@(P<0.05) Vs.* BARM; $*(P<0.05) Vs.* GSM; ns*(P<0.05)* non-significant}

# CHAPTER 6

Fibrosis is defined as an excessive accumulation of extra cellular matrices (ECM), that can result from either imbalance between excessive synthesis of fibrotic components or by impaired degradation of these proteins. The adipose tissue of obese rodents is characterized by increased fibrosis and an upregulation of ECM components. Importantly, visceral adipose tissue fibrosis in obese patients was recently thought to constitute a new mechanism in the development of insulin resistance. Collagens I, III, VI, VIII and X are all expressed by the adipose tissue, with types II and IX expressed at very low levels. Increased ECM components have been associated with adipose tissue fibrosis. Meanwhile, in obesity, constant restoration of the ECM through proteolytic degradation using matrix metalloproteinases (MMP) is required [19]. Thus, histopathological studies of liver and adipose tissues were performed. On continuous exposure to HFD, extensive lipid deposition and hepatic ballooning was observed, indicating liver damage and metabolic stress in the hepatocytes (**Figure 33**) [20,21].

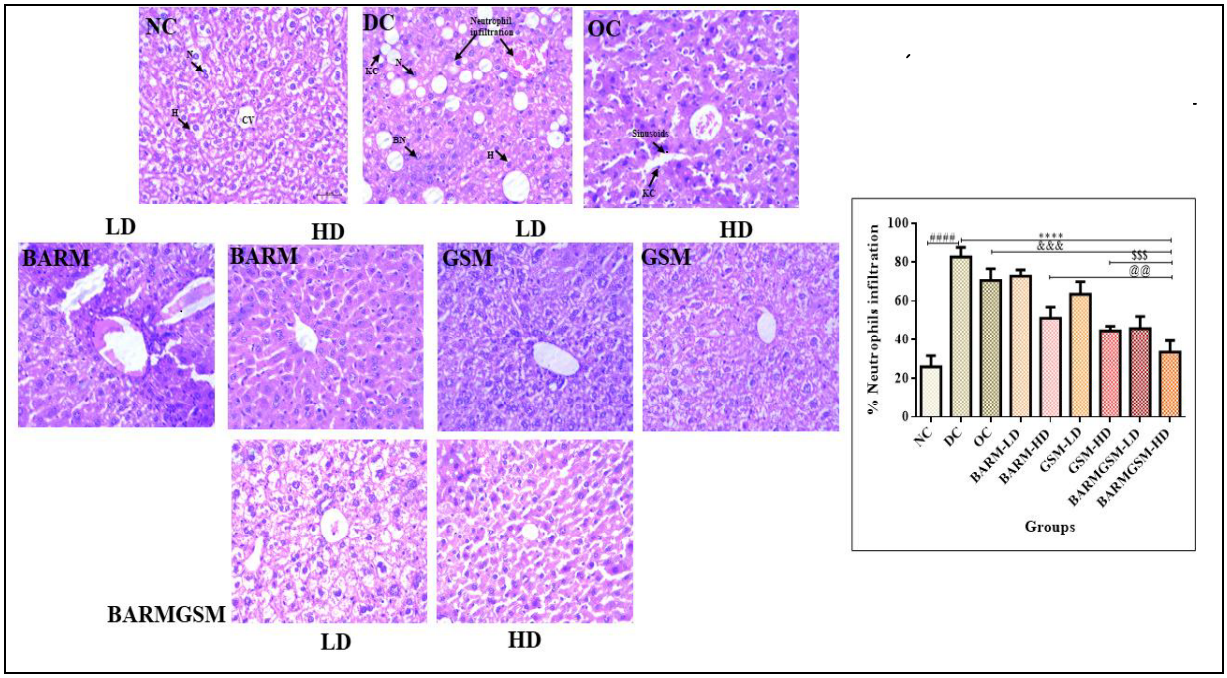


**Figure 33:** H&E staining of liver after treatment with BARM-GSM. (NC- Normal control; DC- Disease control; OC- Orlistat control); CV- Central vein; N-nucleus; H-hepatocytes; BN- Binucleated hepatocytes; KC- Kupffer cells. {*# (P<0.05) Vs.* NC; **(P<0.05) Vs.* DC; &(*P<0.05*) *Vs.* OC; *@(P<0.05) Vs.* BARM; $*(P<0.05) Vs.* GSM; ns*(P<0.05)* non-significant}

Collagen deposition in liver was found to increase followed by an increase in number of Kupffer cells (**Figure 34**) [22].

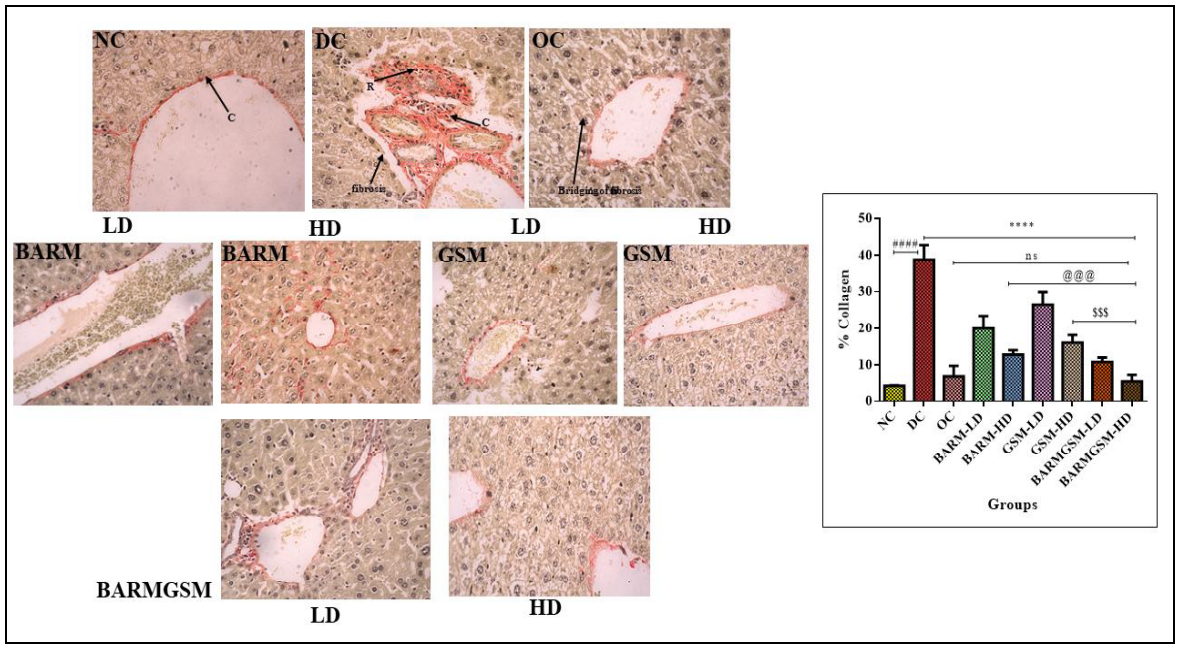


**Figure 34:** Picrosirius red staining of liver after treatment with BARM-GSM. (NC- Normal control; DC- Disease control; OC- Orlistat control); C- Collagen deposition; R- Reticulin fibers {# *(P<0.05) Vs.* NC; **(P<0.05) Vs.* DC; *@(P<0.05) Vs.* BARM; $*(P<0.05) Vs.* GSM; ns *(P<0.05)* non-significant}

Histopathological studies of adipose tissues were performed. Several studies have demonstrated that adipose tissue dysregulation and aberrant adipokine secretion contribute to chronic proinflammatory state. In obesity a predominance of proinflammatory cytokines has been considered. Recent findings suggest that the size of adipocytes is a major modulator of their endocrine function. Hypertrophic adipocytes secrete greater amounts of TNF-α and MCH-1 than normal adipocytes, and this excess secretion has been hypothesized to cause metabolic disorders (**Figure 35**) [23,24].

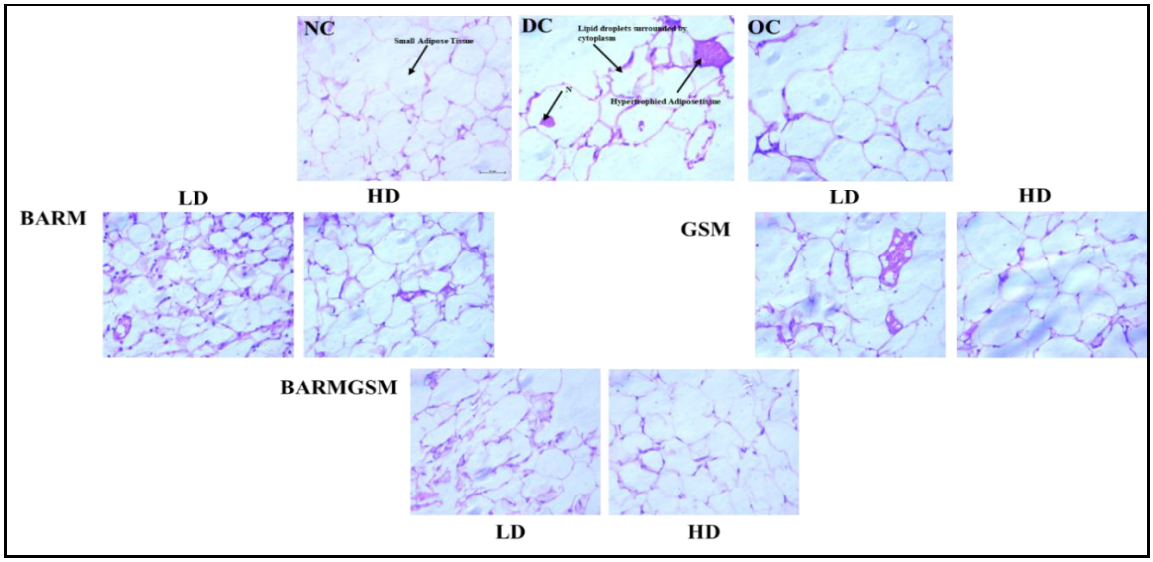


**Figure 35:** H&E staining of adipose tissues after treatment with BARM-GSM. (NC- Normal control; DC- Disease control; OC- Orlistat control)

Previous literatures suggested that berberine (major constituents of *B. aristata*) notably reversed the collagen deposition induced by HFD. Berberine was also found to alleviate adipose tissue fibrosis associated with HFD by activating AMPK activity, inhibiting TGF-β signaling, and attenuating macrophage infiltration, thus improving obesity related adipose tissue fibrosis [19]. On the other hand, epididymal, peritoneal as well as abdominal fat weight were reported to reduce when mice were treated with extracts of *G. sylvestre* [25]. Significant changes ($P<0.05$) such as reduction of hepatic ballooning, neutrophil infiltration and collagen deposition were observed in the BARM-GSM treatment group. Significant changes in neutrophil infiltration and no significant difference in collagen deposition were observed in comparison to the OC group. The combination also showed reduction in the size of the inflamed and hypertrophic adipocytes compared to the DC group, indicating the effective treatment of obesity.

### 6.4 Anti-obesity effect of BARM-TSM in HFD swiss albino mice

Similar approaches were applied in evaluation of BARM-TSM in HFD induced swiss albino mice model. High dose of BARM-TSM (250 mg/kg of BARM+ 500 mg/kg of TSM) showed a significant reduction ($P<0.05$) in bodyweight, adipocytes, and liver weights, indicating that BARM-TSM treatment was effective in reduction of fat deposition. No significant changes were observed when compared to OC group. The BARM-TSM reduced body weight by 39.15% w/w (**Figure 36A**) while 57.81 and 81.71 % w/w reduction of weight of liver and adipocytes were observed (**Figure 36B**).

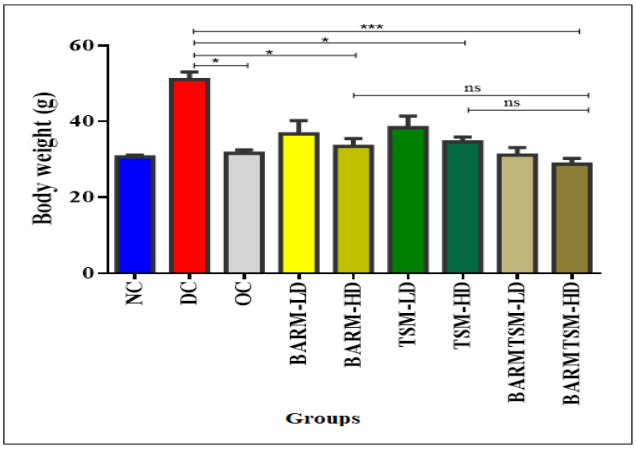


**(A)**

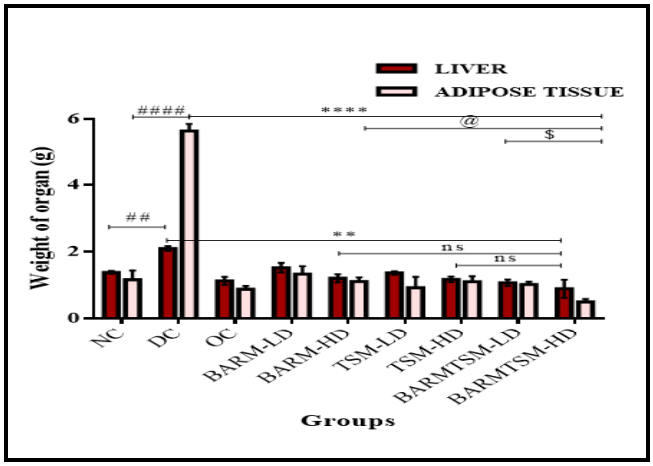


**(B)**

**Figure 36:** Effect of BARM-TSM on (A) bodyweight and (B) liver and abdominal fat content in mice fed with HFD. Results are reported as means ± SEM. {# *(P<0.05) Vs.* NC; **(P<0.05) Vs.* DC; *@(P<0.05) Vs.* BARM; $*(P<0.05) Vs.* TSM; ns *(P<0.05)* non-significant}

BARM-TSM showed a dose-dependent decline in TC (43.65%), and TG (25.12%) once the treatment started. At the end of the study, BARM-TSM significantly reduced (P<0.05) all the biochemical parameters in comparison with the DC group. The results indicate that BARM-TSM was as effective as compared to orlistat, since there was no significant change observed between both the groups (i.e. OC & BARM-TSM-HD). It also significantly increased (P<0.05) serum HDL levels (25.38%) as that of orlistat. LDL and VLDL were calculated using the formula mentioned above (**Figure 37**). Such findings were supported by Tokunaga S. *et al.* report that suggested that consumption of green tea lower the levels of serum TC in both men and women [26]. Berberine and palmatine also reduced TC, TG and LDL and increased HDL levels [18,19].

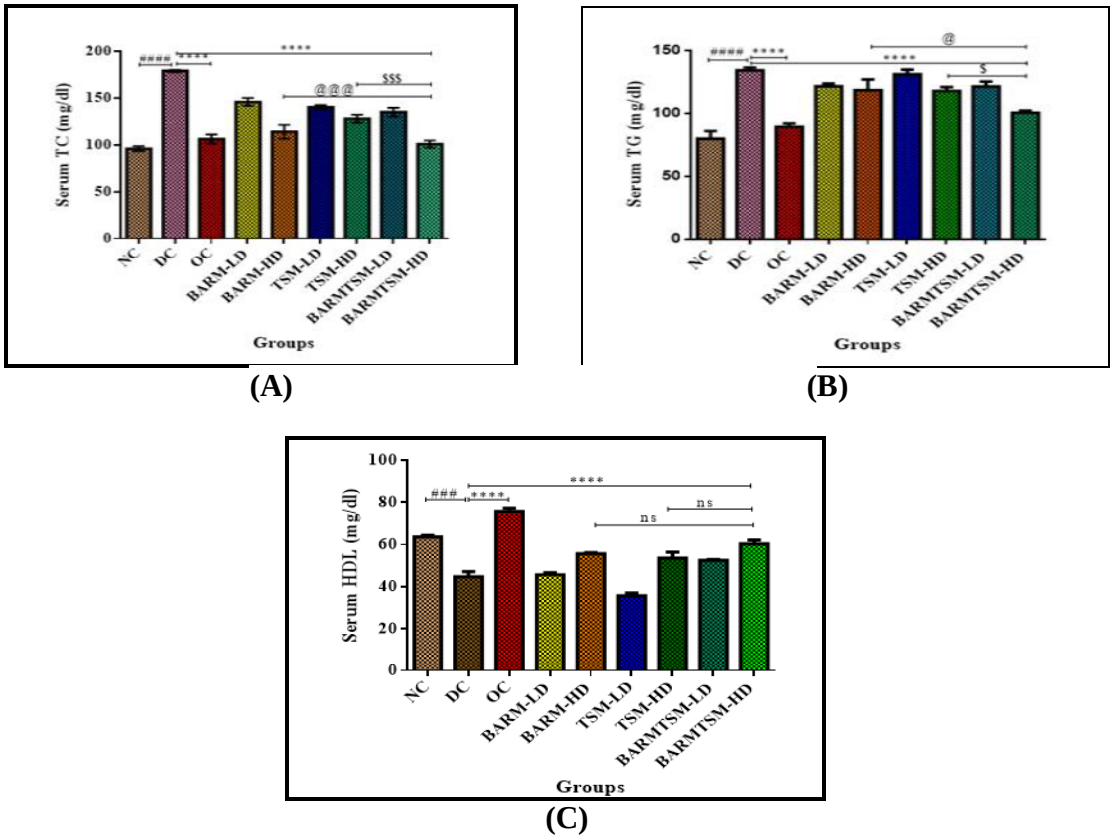


**Figure 37:** Effect of BARM-TSM on serum lipid profile (A) serum TC (B) serum TG and (C) serum HDL. Results are reported as means ± SEM. {*# (P<0.05) Vs.* NC; **(P<0.05) Vs.* DC; *@(P<0.05) Vs.* BARM; $*(P<0.05) Vs.* TSM; ns *(P<0.05)* non-significant}

Values of biochemical parameters namely LDL and VLDL are tabulated in **Table 9**.

**Table 9:** Effect of BARM-TSM on lipid profile

| Groups | LDL (mg/dl) | VLDL (mg/dl) |
|---|---|---|
| NC | 16.37 ± 2.71 | 15.99 ± 1.72 |
| DC | 107.32 ± 1.42 | 26.86 ± 1.42 |
| OC | 12.57 ± 2.19 | 17.90± 2.59 |
| BARM-LD | 75.77 ± 3.26 | 24.31 ± 2.12 |
| BARM-HD | 34.60 ± 3.19 | 23.69 ± 1.46 |
| TSM-LD | 78.25 ± 2.34 | 26.24 ± 1.77 |
| TSM-HD | 50.69 ± 3.98 | 23.59 ± 2.31 |
| BARM-TSM-LD | 58.01 ± 1.34 | 24.30 ± 0.78 |
| BARM-TSM-HD | 29.28 ± 1.97 | 20.11 ± 1.08 |

All the values are expressed as mean± S.E.M (n=6)

To understand, the anti-obesity mechanism of BARM-TSM, fecal TG were analyzed. The low and high dose of individual as well as the combination possessed significant fecal TG levels as

compared to DC (P<0.05). The elevated TG levels in feces confirm that the BARM-TSM exhibited potent anti-obesity activity *via* PL inhibition (**Figure 38**). Significant changes have been observed in fecal TG levels when BARM-TSM-HD treated group was compared to DC and OC groups.

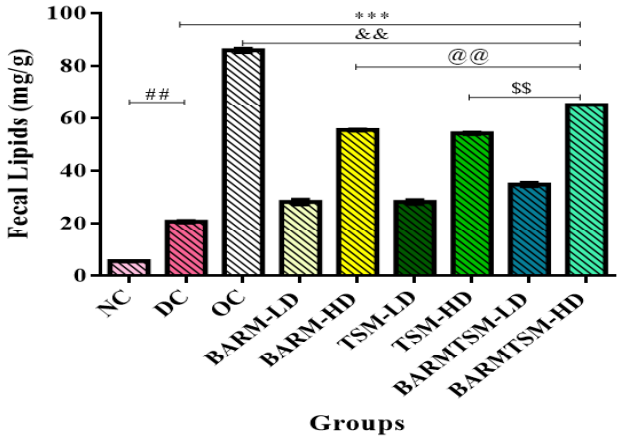


**Figure 38:** Fecal triglyceride levels determined after treatment with BARM-TSM. {# *(P<0.05) Vs.* NC; **(P<0.05) Vs.* DC; &(*P<0.05*) *Vs.* OC; *@(P<0.05) Vs*. BARM; $*(P<0.05) Vs.* TSM; ns *(P<0.05)* non-significant}

Previous literature indicated that epigallocatechin gallate (EGCG) a major constituent of *T. sinensis* extract decreased obesity and epididymal white adipose tissue weight in mice *via* partially activation of AMPK [27]. Other reports suggested that green tea extract rich in catechins such as EGCG inhibited proliferation of fibroblasts, to reduce collagen deposition in liver [28,29]. As stated in previous section berberine causes reduction in collagen deposition and size of adipocytes [16]. Significant changes (P<0.05) were observed such as reduction of hepatic ballooning and neutrophil infiltration in the treatment group (BARM-TSM-HD) when compared with DC and OC groups (**Figure 39**). No significant changes were observed in collagen deposition in the corresponding treatment groups as compared to OC group (**Figure 40**).

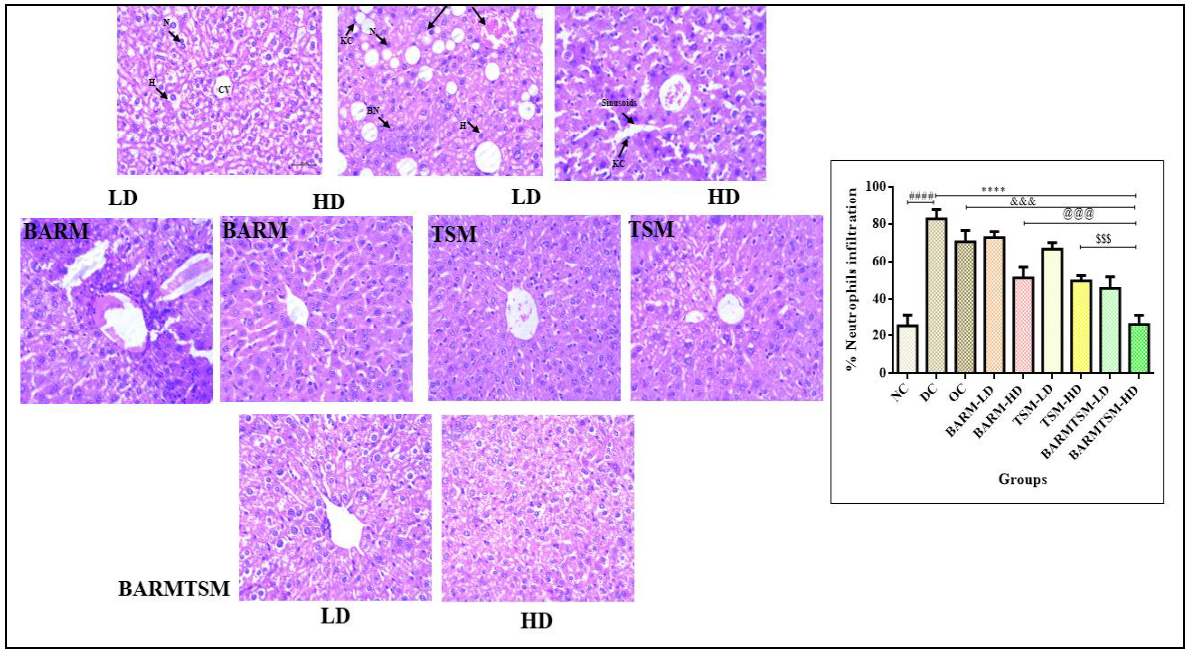


**Figure 39:** H&E staining of liver after treatment with BARM-TSM.(NC- Normal control; DC- Disease control; OC- Orlistat control); CV- Central vein; N-nucleus; H-hepatocytes; BN- Binucleated hepatocytes; KC- Kupffer cells. {# *(P<0.05) Vs.* NC; **(P<0.05) Vs.* DC; &(*P<0.05*) *Vs.* OC; *@(P<0.05) Vs.* BARM; $*(P<0.05) Vs.* TSM; ns *(P<0.05)* non-significant}

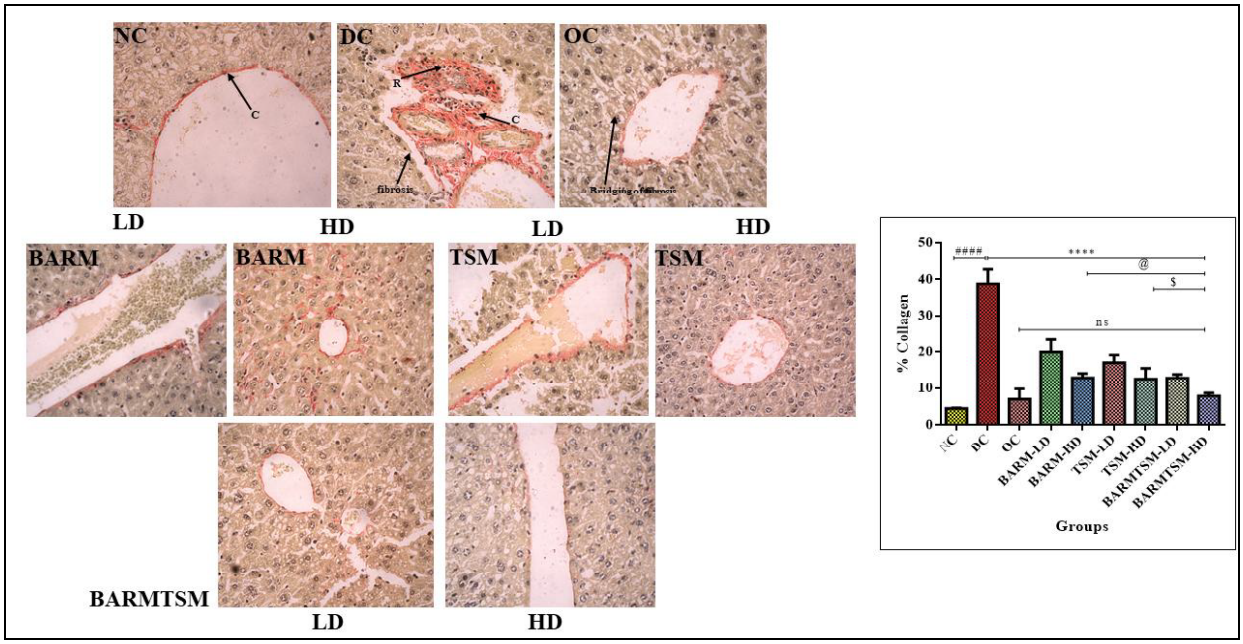


**Figure 40:** Picrosirius red staining of liver after treatment with BARM-TSM. (NC- Normal control; DC- Disease control; OC- Orlistat control); C- Collagen deposition; R- Reticulin fibers. {# *(P<0.05) Vs.* NC; **(P<0.05) Vs.* DC; *@(P<0.05) Vs.* BARM; $*(P<0.05) Vs.* TSM; ns*(P<0.05)* non-significant}

BARM-TSM showed reduction in the size of the inflamed and hypertrophic adipocytes compared to the DC group, indicating the effective treatment of obesity (**Figure 41**).

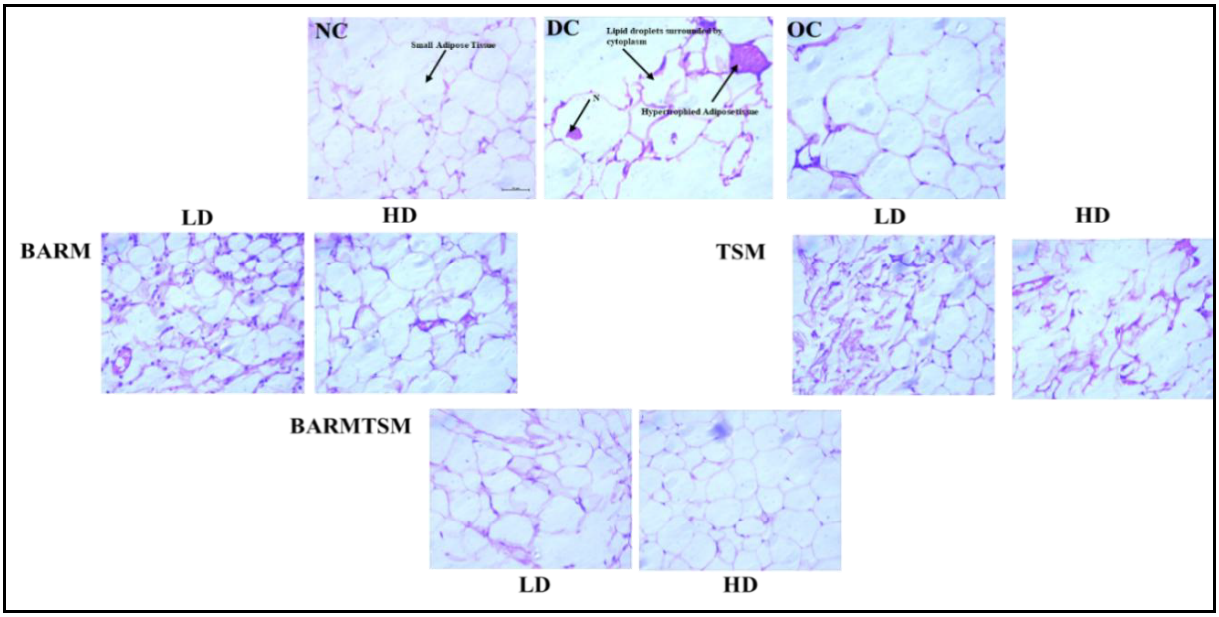


**Figure 41:** H&E staining of adipose tissues after treatment with BARM-TSM. (NC- Normal control; DC- Disease control; OC- Orlistat control).

In conclusion, based on the above *in vitro* results four potent compositions gained attention as they exhibited PL inhibition at higher percentage. Further, the evaluation of these compositions suggested the $cIC_{50}$ of BARM-GSM (5.05 ± 1.05 µg/ml) and BARM-TSM (10.63 ± 0.59 µg/ml) were lesser when compared to GSM-TSM (11.49 ± 0.45 µg/ml) and AMM-PLM (13.55 ± 0.21µg/ml). Thus, the formers were further tested on HFD induced Swiss albino mice model of obesity. Both high doses of BARM-GSM (650 mg/kg) and BARM-TSM (750 mg/kg) showed synergistic effect in *in vivo* studies that reduced the body weight and lipid profile when compared with DC group. Dose-dependent significant changes were observed such as reduction of collagen deposition, neutrophil infiltration in the liver, hepatic ballooning and reduction in the size of the inflamed and hypertrophic adipocytes in the high dose of BARM-GSM and BARM-TSM treated groups as compared to the DC group. The significant presence of TG in fecal samples of mice treated with high dose of BARM-GSM and BARM-TSM further confirmed the anti-obesity effect through PL inhibition.

**References**


1. Foucquier J, Guedj M. Analysis of drug combinations: current methodological landscape. *Pharmacology Research & Perspectives*. 2015;3(3):149-160.
2. Chou T-C. Drug combination studies and their synergy quantification using the Chou-Talalay method. *Cancer Research*. 2010;70(2):440-446.
3. Sengupta P, Raman S, Chowdhury R, *et al.* Evaluation of apoptosis and autophagy inducing potential of *Berberis aristata*, *Azadirachta indica*, and their synergistic combinations in parental and resistant human osteosarcoma cells. *Frontiers in Oncology*. 2017; 11:7(296):1-17.
4. Huang R-y, Pei L, Liu Q, *et al.* Isobologram analysis: A comprehensive review of methodology and current research. *Frontiers in Pharmacology*. 2019; 29:10(1222):1-12.
5. Sridhar S, Sengupta P, Paul AT. Development and validation of a new HPTLC method for quantification of conophylline in *Tabernaemontana divaricata* samples obtained from different seasons and extraction techniques: Insights into variation of pancreatic lipase inhibitory activity. *Industrial Crops and Products*. 2018;111:462-470.
6. George G, Sridhar SNC, Paul A. Investigation of synergistic potential of green tea polyphenols and orlistat combinations using pancreatic lipase assay-based synergy directed fractionation strategy. *South African Journal of Botany*. 2020;135:50-57.
7. Lutz TA, Woods SC. Overview of animal models of obesity. *Current protocols in Pharmacology*. 2012;5:1-22.
8. Reddy RM, Latha PB, Vijaya T, *et al.* The saponin-rich fraction of a *Gymnema sylvestre* R. Br. aqueous leaf extract reduces cafeteria and high-fat diet-induced obesity. *Zeitschrift für Naturforschung C*. 2012;67(1-2):39-46.
9. Al-Romaiyan A, King AJ, Persaud SJ, *et al.* A novel extract of *Gymnema sylvestre* improves glucose tolerance *in vivo* and stimulates insulin secretion and synthesis *in vitro*. *Phytotherapy Research*. 2013;27(7):1006-1011.
10. Liu C, Guo Y, Sun L, *et al.* Six types of tea reduce high-fat-diet-induced fat accumulation in mice by increasing lipid metabolism and suppressing inflammation. *Food and Function*. 2019;10(4):2061-2074.
11. Chan PC, Ramot Y, Malarkey DE, *et al.* Fourteen-week toxicity study of green tea extract in rats and mice. *Toxicology and Pathology*. 2010;38(7):1070-1084.

12. Hu Y, Davies GE. Berberine inhibits adipogenesis in high-fat diet-induced obesity mice. *Fitoterapia*. 2010;81(5):358-366.
13. Long J, Song J, Zhong L, *et al.* Palmatine: A review of its pharmacology, toxicity and pharmacokinetics. *Biochimie*. 2019;162:176-184.
14. Tian X, Zhang Y, Li H, *et al.* Palmatine ameliorates high fat diet induced impaired glucose tolerance. *Biological Research*. 2020;53(1):1-12.
15. Chaudhari HS, Bhandari U, Khanna G. Preventive effect of embelin from *Embelia ribes* on lipid metabolism and oxidative stress in high-fat diet-induced obesity in rats. *Planta Medica*. 2012;78(7):651-657.
16. Karavia EA, Papachristou DJ, Liopeta K, *et al.* Apolipoprotein A-I modulates processes associated with diet-induced nonalcoholic fatty liver disease in mice. *Molecular Medicine.* 2012;18(6):901-912.
17. Derosa G, D'Angelo A, Bonaventura A, *et al.* Effects of berberine on lipid profile in subjects with low cardiovascular risk. *Expert Opinion on Biological Therapy*. 2013;13(4):475-82.
18. Ma H, Hu Y, Zou Z, *et al.* Antihyperglycemia and antihyperlipidemia effect of protoberberine alkaloids from *Rhizoma coptidis* in HepG2 cell and diabetic KK-Ay mice. *Drug Development Research.* 2016;77(4):163-170.
19. Wang L, Ye X, Hua Y, *et al.* Berberine alleviates adipose tissue fibrosis by inducing AMP-activated kinase signaling in high-fat diet-induced obese mice. *Biomedicine & Pharmacotherapy*. 2018;105:121-129.
20. Lee YS, Cha BY, Yamaguchi K, *et al.* Effects of Korean white ginseng extracts on obesity in high-fat diet-induced obese mice. *Cytotechnology*. 2010;62:367-376.
21. Mujawdiya PK, Sharma P, Sharad S, *et al.* Reversal of increase in intestinal permeability by *Mangifera indica* seed kernel extract in high-fat diet-induced obese mice. *Pharmaceuticals*. 2020;13(8):190-210.
22. Hassan N, Soliman G, Okasha E, *et al.* Histological, immunohistochemical, and biochemical study of experimentally induced fatty liver in adult male albino rat and the possible protective role of pomegranate. *Journal of Microscopy and Ultrastructure*. 2018;6(1):44-55.
23. Melo TS, Lima PR, Carvalho KMMB, *et al.* Ferulic acid lowers body weight and visceral fat accumulation via modulation of enzymatic, hormonal and inflammatory changes in a mouse

model of high-fat diet-induced obesity. *Brazilian Journal of Medical and Biological Research*. 2017;50 (1): e5630

24. Bremer AA, Jialal I. Adipose tissue dysfunction in nascent metabolic syndrome. *Journal of Obesity*. 2013;2013 (10):1-8.
25. Kim H-J, Hong S-H, Chang S-H, *et al.* Effects of feeding a diet containing *Gymnema sylvestre* extract: Attenuating progression of obesity in C57BL/6J mice. Asian Pacific *Journal of Tropical Medicine*. 2016;9(5):437-444.
26. Tokunaga S, White IR, Frost C, *et al.* Green tea consumption and serum lipids and lipoproteins in a population of healthy workers in Japan. *Annals Epidemiology*. 2002;12(3):157-165.
27. Li F, Gao C, Yan P, *et al.* EGCG reduces obesity and white adipose tissue gain partly through AMPK activation in mice. *Frontiers in Pharmacology*. 2018;9:1-9.
28. Tipoe GL, Leung TM, Liong EC, *et al.* Epigallocatechin-3-gallate (EGCG) reduces liver inflammation, oxidative stress and fibrosis in carbon tetrachloride (CCl4)-induced liver injury in mice. *Toxicology*. 2010;273(1):45-52.
29. Sakata R, Nakamura T, Torimura T, *et al.* Green tea with high-density catechins improves liver function and fat infiltration in non-alcoholic fatty liver disease (NAFLD) patients: A double-blind placebo-controlled study. *Internation Journal of Molecular Medicine*. 2013;32(5):989-994.